# Proposal for AGS

October 6, 2001


**From:** Imai, K. (Kyoto University)
Nakazawa, K. (Gifu University)
Tamura, H. (Tohoku University)


**Title:** Systematic Study of Double Strangeness System by an Emulsion-Counter Hybrid Method

**Beam:** 1.7 GeV/c $K^-$; $2\times10^5$ $K^-$/spill(4.1sec) with $K^-/\pi^- \geq 9$

**Beam Line:** 2 GeV/c $K^-$ beam line

**Detectors:** Nuclear emulsion, double-sided Si strip detectors, Ge detectors (Hyperball), Scintillating fiber detector, KURAMA (or USHIWAKA) magnet, drift chambers, plastic counters

**Time Requested:** First year; 100 hours for detector tune
100 hours for beam tune
550 hours for beam exposure
Second year; 100 hours for detector tune
550 hours for beam exposure

# 1 Introduction

The purpose of the proposed experiment is a systematic study of double strangeness ($S$=-2) systems via nearly 100 nuclear samples and a few hundreds of $\Xi^-$ atomic X-ray events.

The evidence of a double strangeness nucleus in the emulsion following $\Xi^-$ capture at rest was reported more than thirty years ago [1, 2, 3]. At KEK, we carried out an emulsion-counter hybrid experiment (E176) to observe double strangeness nuclei and/or $H$ dibaryon. Among nearly 80 stopping $\Xi^-$ events extracted from 2000 ($K^-$,$K^+$) reaction events, existence of the ground state of double strangeness nuclei was confirmed by observing cascade weak decay [4]. This event, however, did not allow us to derive the $\Lambda\Lambda$ interaction energy ($\Delta B_{\Lambda\Lambda}$) uniquely; $\Delta B_{\Lambda\Lambda}$ was obtained to be either $-4.9\pm0.7$ MeV (repulsive $\Lambda\Lambda$ interaction) or $+4.9\pm0.7$ MeV (attractive interaction).

The E373 experiment at KEK started to solve the question about the $\Lambda\Lambda$ interaction given by E176, to confirm the findings of E176 with better accuracy, and to provide new discoveries about double strangeness nuclei [5]. In E373, the quasi-free '$p$'($K^-$,$K^+$)$\Xi^-$ reactions were induced in the diamond ($^{12}$C) target located upstream of the emulsion. Some of the $\Xi^-$ hyperons were stopped in the emulsion stack. The high precision tracking detector, micro fiber-bundle tracker [6], was placed between the target and the emulsion to guide the $\Xi^-$ tracks into the first emulsion plate. Since the ionization of the $\Xi^-$ hyperons with a momentum of $\sim 0.5$ GeV/c is several times larger comparing minimum ionizing particles, tracing of the $\Xi^-$ tracks is easier and faster than tracing of $K^+$ tracks done in E176. The automated scanning system was also successfully developed for $\Xi^-$ track tracing in the emulsion of E373 to reduce the time for emulsion analysis. In E373, we can obtain $10^3$ stopping $\Xi^-$ events which is ten times larger number than that presented by E176. The beam exposure was finished in 2000, and the analysis is in progress. Though we have finished analysis of only 11 % data, an event showing the decay topology of the twin single $\Lambda$ hypernuclei [7] and an ${}^{6}_{\Lambda\Lambda}$He double hypernucleus event [8] were successfully detected. In particular, the latter is a beautiful event which was uniqely identified and confirmed for the first time that the $\Lambda\Lambda$ interaction was weakly attractive. This method has been thus proved to be promising for the study of nuclei with double stragness system. Further studies with ten times higher statistics in the proposed experiment will reveal the properties of double strangeness system in detail and provide us a clue to understand the baryon-baryon interactions and the nuclear matter with multi-strangeness.

In strangeness nuclear physics, another type of new experiments, hypernuclear $\gamma$ spectroscopy, has recently been developed. In 1998 we constructed a germanium (Ge) detector array (Hyperball) and successfully observed hypernuclear $\gamma$ transitions in ${}^{7}_{\Lambda}$Li and ${}^{9}_{\Lambda}$Be in KEK E419 and BNL E930 with a few keV resolution, which is better by two or three orders of magnitude than the conventional hypernuclear spectroscopy. The results provided unambiguous information of the strengths of the spin-spin [9] and the spin-orbit interactions [10] between a $\Lambda$ and a nucleon, as well as to confirm the hypernuclear shrinking effect [11]. This

new technique can be also applied to detection of $\Xi^-$ atomic X rays and to measure their energy shifts, which will provide precious information on the $\Xi N$ interaction.

We use almost pure $K^-$ beam of the 2 GeV/c K-beam line (D6) in the proposed experiment. The ($K^-$,$K^+$) reaction, $K^- + {}'p' \rightarrow K^+ + \Xi^-$, from a carbon target is detected with the spectrometer system using KURAMA or USHIWAKA magnet from KEK. The target and the emulsion system is almost the same as in E373. A new high position resolution detector, double-sided Si strip detector(DSSD), is placed between the target and the emulsion stack and to tag the $\Xi^-$ hyperons produced in the target and stopped in the emulsion. To condense events associated with stopping $\Xi^-$ hyperons, an additional DSSD is set just downstream of the emulsion. Scintillating fiber (SCIFI) blocks which surround the emulsion is used to detect $\pi^-$ from decays of the hyperfragments and other particles. These detectors will reduce the number of events to be scanned in emulsion. High purity kaon beam at D-line ($K/\pi$ ratio of KEK K2-line is 1/4 at most), advanced detectors and automated scanning system enable us to obtain ten times more events than E373 within a few years of data analysis.

We install Hyperball around the target to detect $\Xi^-$ atomic X rays, where stopped $\Xi^-$ events are clearly identified from the emulsion analysis. Hyperball is now working at BNL for E930 run. A few hundreds of events of both of Ag-$\Xi^-$ atomic X rays and Br-$\Xi^-$ atomic X rays will be detected, and their energy shifts will be measured with 0.3 keV accuracy.

By the above experimental condition to achieve statistics with ten times more than that of E373, we can systematically measure a nuclear mass number ($A$) dependence of the $\Lambda\Lambda$ interaction energy from at least several kinds of $S$=-2 nuclides in nearly 100 samples to be identified as $S$=-2 nuclei. We can thus provide a chart of $S$=-2 nuclides for the first time. The decay mode of $S$=-2 nuclei can also be systematically measured for the first time. Existence of the bound $H$ particle is now very unlikely after many experimental efforts. However, there still remain a possibility of the $H$ as a resonance near the $\Lambda\Lambda$ threshold. It is theoretically suggested that the $H$ dibaryon like state may possibly exist as a mixing state of $\Lambda\Lambda$, $\Xi N$ and $\Sigma\Sigma$ in a nucleus. Experimental results of the $A$ dependence of $\Delta B_{\Lambda\Lambda}$ and the decay mode can give definitive information on how the $H$ dibaryon exists in $S$=-2 nuclei. We will also search for the $H$ resonance in the $\Lambda\Lambda$ invariant mass spectrum which can be obtained mainly by a scintillation fiber detectors.

The energy measurement of X rays from the decay of $S$=-2 system is carried out for the first time. We expect that several hundreds of X ray events from $\Xi^-$-Ag and $\Xi^-$-Br atoms will clarify the $\Xi^-$-nucleus potential and to reveal the $\Xi^- N$ interaction.

This proposal is based on the experience of KEK-E176, E224, E373, E419 and BNL-E813, E885, E930. We combine their newly-developed but already-established techniques of hybrid emulsion method, scintillating fiber detectors, diamond target, high-rate Ge detectors, etc. The collaborators are mainly from the members of those experiments.

# 2 Physics

## 2.1 Double strangeness nuclei and $H$ dibaryon

The double Λ hypernuclei, $H$ nuclei and Ξ hypernuclei are all double strangeness nuclei. Which is the ground state? The conventional idea is that it is double Λ hypernuclei. However, it is not trivial, since we do not know the mass of the $H$ particle, $H$ nucleon interaction and Ξ nucleon interaction, experimentally. Theoretically, the baryon-baryon interaction in the $S$=−2 state can be attractive at short distance, compared with the repulsive core of the nucleon-nucleon interaction. That is the reason why the $H$ dibaryon can be a stable 6-quark state [12]. Therefore, the double strangeness nuclei can be quite different nuclei from the ordinary nuclei or Λ hypernuclei. The strange quark matter is an extreme example of these discussion. However, very little is known about the double strangeness nuclei, experimentally. One of the most important thing for the study of double strangeness nuclei is to identify the nuclear species and measure their masses (binding energies).

Recently, we have succeeded in observing an event which is uniquely identified as *Lambpha*, ${}^{6}_{\Lambda\Lambda}$He double Λ hypernucleus, in the ground state [8]. The photographic image and a schematic drawing of the event named "NAGARA" is shown in Fig. 1. The formation and the decay of *Lambpha* was interpreted as: $\Xi^-+{}^{12}\mathrm{C} \rightarrow {}^{6}_{\Lambda\Lambda}\mathrm{He}+{}^{4}\mathrm{He}+t$, ${}^{6}_{\Lambda\Lambda}\mathrm{He} \rightarrow {}^{5}_{\Lambda}\mathrm{He}+\pi^-+p$, ${}^{5}_{\Lambda}\mathrm{He} \rightarrow p+d+2n$ *etc.* The binding energy of the two Λ hyperons ($B_{\Lambda\Lambda}$) provides the ΛΛ interaction energy $\Delta B_{\Lambda\Lambda}$ as follows,

$$\Delta B_{\Lambda\Lambda}({}^{A}_{\Lambda\Lambda}\mathrm{Z}) = B_{\Lambda\Lambda}({}^{A}_{\Lambda\Lambda}\mathrm{Z}) - 2B_{\Lambda}({}^{A-1}_{\Lambda}\mathrm{Z}).$$

$\Delta B_{\Lambda\Lambda}$ provides important information on the ΛΛ interaction. $B_{\Lambda\Lambda}$ and $\Delta B_{\Lambda\Lambda}$ ( ${}^{6}_{\Lambda\Lambda}$He) from the NAGARA event were obtained as 7.25 ± 0.19 $^{+0.18}_{-0.11}$ MeV and 1.01 ± 0.20 $^{+0.18}_{-0.11}$ MeV, respectively, using the most probable $\Xi^-$ binding energy of 0.13 MeV which is the level energy of ${}^{12}$C atomic 3$D$ state [13, 14]. This value demonstrates the ΛΛ interaction is attractive but very weak rather than 4∼5 MeV which has been believed for forty years. In two old emulsion events [1, 2] [4] and our $Demachi-Yanagi$ event obtained by E373 [15, 16], there is a possibility that single hypernucleus was produced in excited states, and $\Delta B_{\Lambda\Lambda}$ cannot be uniquely extracted. If excited states are taken into account, their values of $\Delta B_{\Lambda\Lambda}$ do not contradict with our new result. However, the disagreement between our $\Delta B_{\Lambda\Lambda}({}^{6}_{\Lambda\Lambda}\mathrm{He})$ and that reported in Ref. [3] confirms the doubts on the authenticity of the event in [3].

The binding energy $B_{\Lambda\Lambda}$ of the ground state provides the lower bound of the mass of the possible $H$ particle, since the double strangeness nuclei can decay into the $H$ and residual nucleus by the strong interaction if the mass of the $H$ is smaller than ( $2M_{\Lambda} - B_{\Lambda\Lambda}$ ).

For more than a decade, many experiments were carried out to search for the $H$ particle in the mass range from below $NN$ threshold to over the mass of two Σ hyperons. However, none of them has reported definitive observation of the bound $H$ particle and/or its resonance

state yet [17]. Recently a possible resonance just above the threshold has been suggested in the $\Lambda\Lambda$ invariant mass spectrum [18]. In the proposed experiment, we can study the $\Lambda\Lambda$ invariant mass spectrum about 100 times more statistics than the previous data. Even with the new E373 event, there still remains a small window for the mass of the $H$ particle, $2M(\Lambda) \geq M(H) \geq 2M(\Lambda) - 7.25$ MeV, but the existence of the deeply-bound $H$ dibaryon appears very unlikely.

Two cases can be considered for the bound state of $S$=-2 nuclear system in relation with the $H$, namely,

case 1.: $\Lambda\Lambda$ nucleus, or

case 2.: $H$-nucleus state with a loosely-bound $H$.

In reality, they can be mixed as well as with $\Xi N$ and $\Sigma\Sigma$ states. Yamada et al. calculated the ground state for the case 2. of the system, core[$^8$Be] + (3q) + (3q) [19], based on Quark Cluster Model. They found a "loosely-bound $H$ dibaryon state" which is the flavor SU(3)×SU(3) singlet state but consists of two loosely bound baryons having a strongly-mixed $\Lambda\Lambda$-$\Xi N$-$\Sigma\Sigma$ function.

How can we distinguish the above two cases?

One way is to measure the nuclear mass number ($A$) dependence of the binding energies, especially $\Delta B_{\Lambda\Lambda}$. If the ground state of $S$=-2 system consists of the $H$ particle made of six quarks, '$\Delta B_{\Lambda\Lambda}$' is expected to be same for different nuclear species. However, in the case of the two baryonic state (case 1) $\Delta B_{\Lambda\Lambda}$ may be not constant when the core nucleus is changed. Yamada et al. showed that $\Delta B_{\Lambda\Lambda}$ for ${}^{14}_{\Lambda\Lambda}$C becomes $\sim$ 1 MeV larger than that for ${}^{6}_{\Lambda\Lambda}$He [20]. The other way is a measurement of the decay mode of the $S$=-2 ground states. In the case of $H$-nuclei, it is expected to decay into $\Sigma N$ and $\Lambda N$ as well as $\Lambda N\pi$ at large branching ratio. Because of the large Q-value, $\Sigma N$ and $\Lambda N$ decays can be identified in this experiment.

Theoretical studies on the binding energy of $H$-nuclei as well as double $\Lambda$ nuclei and non-mesic decays of $S$=-2 have just begun. Together with these theoretical studies, data from the proposed experiment will answer the question. The mesonic decay $\pi^-/\pi^0$ ratio will also provide important information on the $S$=-2 ground state [20].

The present experiment expects to obtain $10^4$ stopping $\Xi^-$ events in the emulsion. Among those events, we expect to identify about 100 double strangeness nuclei. A chart of nuclides with double strangeness will be made for the first time. The masses and binding energies will be obtained without any ambiguity for, at least, several nuclides. If we observe the same nuclide but with 'different binding energy', it provides the first observation of an excited state of $S$=-2 nuclei.

The $A$ dependence of the $\Lambda\Lambda$ interaction energy is, thus, provided for the first time. We can also investigate decay modes of those $S$=-2 nuclei and provide information on their structure. The measurements of the $A$ dependence of $\Delta B_{\Lambda\Lambda}$ and the decay modes of $S$=-2 nuclei will answer the question on existence of the $H$ dibaryon near threshold, which may possibly appear as a mixed state with $\Lambda\Lambda - \Xi N - \Sigma\Sigma$.

## 2.2 $\Xi^-$ atoms and $\Xi$-nucleus interaction

In order to understand the properties of the $S$=-2 system, namely, the mixing of $\Lambda\Lambda$-$\Xi N$-$\Sigma\Sigma$ and possibly also with $H$ dibaryon state, study of $\Xi^-$-nucleus interaction is of particular importance.

A stopped $\Xi^-$ is captured by an atom in the emulsion (C, N, O, Ag, or Br). It is firstly captured by a highly excited atomic orbit and transferred into lower orbits by Auger effect and radiative transitions. Finally the $\Xi^-$ is absorbed by the nucleus via strong interaction when the atomic orbit and the nucleus has a large overlap. We can obtain information on the $\Xi$-nuclear interaction from the last radiative transition, because the $\Xi^-$-nucleus interaction affects the energy and the width of the atomic level in which the nuclear capture takes place, as well as the yield of the transition (the branching ratio of the upper level going to the radiative decay or to the nuclear absorption).

The $\Xi$-nucleus interaction was studied by the $^{12}$C($K^-$,$K^+$) reaction in KEK E176, E224 and BNL E885 [21]. Although they did not observe $\Xi$ hypernuclear peaks, the well depth of the $\Xi$-nucleus potential was found to be weakly attractive (around -14 MeV assuming the Woods-Saxon shape) from the spectrum shape. But the potential shape may not be simply proportional to the nuclear density, as is discussed in the case of $\Sigma$ nucleus potential [22], depending on the 2-body $\Xi N$ interaction.

Since the X-ray data provide information of the nuclear potential (both of real and imaginary parts) at outer part, combination of X-ray data with two or more atomic numbers together with the previous ($K^-$,$K^+$) data will allow us to determine both of the depth and the shape of the $\Xi$-nucleus potential.

In the proposed experiments, we cannot measure the widths smaller than 2 keV, while we can obtain the X-ray yields which also give information on the imaginary part of the potential.

According to theoretical calculation by Batty, Friedman and Gal [14, 23], the shift and the yield are predicted as listed in Table 1. Here the calculation was performed for two types of potentials with different shapes but consistent with the previous ($K^-$,$K^+$) data. Even in the case 1 ($t\rho$ potential, proportional to nuclear density), where the effect of the potential at the outer part is smallest, 0.3-0.7 keV shifts are predicted. It is within accuracy of our measurement.

In addition, by detecting photons for $\Xi^-$ absorption events, we may be able to detect $\gamma$ transitions in double $\Lambda$ hypernuclei as well as $\Xi$ atomic X rays. Expected numbers of such $\gamma$ rays are very small in the proposed experiment, but our measurement will provide a good test data for future experiments of $\gamma$ spectroscopy of double $\Lambda$ hypernuclei.

Information on $\Xi^-$ nucleus potential can also be obtained from the decay of the $\Xi^-$-nucleus system; if all the emitted particles are well identified, the mass of the parent $\Xi^-$ bound system can be obtained. If two $\Lambda$ hyperons are captured by different fragments, namely, two single-$\Lambda$ hypernuclei are produced, after the $\Xi^-$ is absorbed, then we can determine the

| $Z(n,l)$ | $E$ (keV) | shift (keV) | width (keV) | $R_X$ |
|---|---|---|---|---|
| Ag (8,7)→(7,6) | | | | |
| case 1 | 370.45 | 0.28 | 0.15 | 0.88 |
| case 2 | | 3.3 | 0.79 | |
| Br (7,6)→(6,5) | | | | |
| case 1 | 315.5 | 0.73 | 0.44 | 0.67 |
| case 2 | | 5.5 | 1.74 | |

Table 1: Calculated shifts, widths, and yield ratio $R_X$ of $\Xi^-$ X rays on Ag and Br. Case 1 is calculated assuming the potential shape to be the same as the nuclear density ($t\rho$ potential). Case 2 is calculated using the potential derived from G matrix calculation with the $\Xi N$ interaction in the Nijmegen D model but corrected to reproduce the potential depth of about 14 MeV.

mass of the $\Xi^-$ bound system because we know binding energies of all kinds of light single $\Lambda$ hypernuclei.

In E176, two such events, so-called twin single $\Lambda$ hypernuclei, where two single hyperfragments are emitted back to back from the $\Xi^-$ stopping points were found. One was interpreted as $\Xi^-$ C-atomic state with the binding energy of $0.53 \pm 0.22$ MeV [24] and the other as possible $\Xi^-$ C-nucleus with the binding energy of $3.70 \pm 0.19$ MeV [25], although other interpretations were not excluded.

When $\Xi^-$ is captured by a light emulsion nucleus (C,N,O), then it is mainly absorbed by $3D$ atomic orbit. But theoretical calculations show that the absorption takes place at $2P$ orbit for a few percent probability, in which case a large binding energy of $\Xi$ (of the order of MeV) may be observed.

In the proposed experiment, we will be able to observe a few hundred events of this kind and to get binding energies of deeply-bound $\Xi^-$ nuclear states more reliably.

# 3 Experimental Method

## 3.1 Introduction

We propose an emulsion-counter hybrid method to study double strangeness system produced from $\Xi^-$ stopping points in the emulsion. The double strangeness nuclei are identified by the characteristic cascade weak decay. Short tracks of hyperfragments and their decay vertices are extensively studied in the emulsion together with other decay particles. The emulsion is surrounded by scintillating fiber detectors which detect long tracks such as $\pi^-$ from hyperfragments, decay particles from $H$ dibaryon, and decay particles of $\Lambda$ from the weak interaction such as $\Lambda\Lambda \to \Lambda N$. Ge detectors measure X rays from $\Xi^-$ atoms formed

by $\Xi^-$ capture at rest.

The quasi-free reaction, $K^- + p \rightarrow K^+ + \Xi^-$, from a diamond target is detected by the spectrometer system using KURAMA or USHIWAKA magnet from KEK. Some of $\Xi^-$ hyperons from the target are stopped in the emulsion stack placed downstream of the target. A high precision position detector, double-sided Si strip detector (DSSD), placed between the target and the emulsion is used to identify the tracks of the $\Xi^-$ going to the emulsion. We will set an additional DSSD to recognize that the $\Xi^-$ hyperon does not go through out of the emulsion, to measure the energy of charged particles escaping from the emulsion and, if possible, to locate some vertices in the emulsion by tracing back the tagged $K^+$ or other tracks. In the emulsion, the $\Xi^-$ track is traced down to its stopping point, and the vertices of the stopping $\Xi^-$ events are studied in detail under a microscope to find out a double strangeness system. According to track lengths emitted from the stopping point, the nuclei which captured $\Xi^-$ hyperons are classified to two categories, light elements (C, N, O) or heavy ones (Ag, Br).

The emulsion is very expensive ($8,000 for 1 *liter* including the fee for development). In addition, analysis of the emulsion is time and man-power consuming job, even after we successfully develop a fully automated emulsion scanning system. The experiment is thus designed to save the amount of the emulsion and to make the analysis easier and faster.

## 3.2 Setup of the experiment

The 1.7 GeV/c $K^-$ beam is used for this experiment. We need only $2\times10^5$ $K^-$/spill(4.1sec) as a beam intensity but require a pure $K^-$ beam with the $K^-$/beam ratio of better than 0.9. A schematic drawing of the experimental setup is shown in Fig. 2. The apparatus near the emulsion are also shown in Fig. 3. The time-of-flight counters (T1 - T2) and an aerogel Cherenkov counter (BAC; n=1.03) are used to identify the $K^-$ mesons. A heavy-metal collimator is used to obtain a small sized beam ($10 \times 20$ mm$^2$) at the target. A diamond target sized $1 \times 2$ cm$^2$ and 3cm in length is placed upstream of the emulsion stack. It is used as the $\Xi^-$ production target and as an energy degrader for the $\Xi^-$ hyperons. Two sets of DSSD's are placed between the target and the emulsion stack to measure the angle and position of the $\Xi^-$ hyperons with high precision instead of a fiber-bundle tracking detector which was employed in E373.

The scattered $K^+$ particles are detected with the $K^+$ spectrometer system which consists of a magnet (KURAMA or USHIWAKA from KEK), time-of-flight counters (FTOF-T2), aerogel Cherenkov counters (BVAC, FAC), drift chambers (DC1-3) and trigger counters. The scintillating fiber detectors (SCIFI) are placed up- and downstream of the emulsion stack primarily to measure the energy of $\pi^-$ from the hypernuclei, to detect $\Lambda$ hyperons, and to search for the $H$ resonance.

The Ge detector array (Hyperball) covers the upstream hemisphere of the target and detects $\Xi^-$ atomic X rays around 300-400 keV with an energy resolution of 2.5 keV (FWHM).

Here we use twelve Ge detectors and covers about 15% of the total solid angle. Each Ge detector is surrounded by BGO counters.

## 3.3 $K^+$ Spectrometer

The $K^+$ spectrometer is essentially the same as the one used for E373. The $K^+$ particles are identified by time-of-flight counters and aerogel Cherenkov counters. Almost perfect identification of $K^+$ is possible as shown in the mass spectrum of scattered particles obtained by E373 (Fig. 5).

The momentum of the $K^+$ particle is measured with the magnet (KURAMA or USHIWAKA) and drift chambers. The momentum resolution obtained by E373 is good enough to identify quasi-free $\Xi^-$ production from the carbon target. The acceptable integral beam flux is limited by the amount of emulsion. Therefore, in order to get as many events as possible with a limited amount of the emulsion, detection efficiency of $K^+$ mesons must be as high as possible. It is why we use the KURAMA (or USHIWAKA) magnet, which has a larger acceptance for $K^+$, instead of the 48D48 magnet currently installed at the D6 beam line. The TOF counters will be placed downstream of the DC3. The shorter distance from the target to the TOF counters reduces the inefficiency due to the $K^+$ decay in the spectrometer and increases the acceptance. We expect to obtain an acceptance of 0.20 sr with KURAMA, rather than about 0.10 sr with the 48D48 magnet.

## 3.4 Tracking detectors

### 3.4.1 double-sided Si strip detector (DSSD)

In E373, we used micro fiber-bundle tracking detectors for the $\Xi^-$ tracking from the target to the first plate of the emulsion stack. The detector consists of fine scintillating fibers with a diameter of $\sim$ 40 $\mu$m. The image scanning by human eyes is necessary to find the $\Xi^-$ candidate tracks. In the proposed experiment, however, it is necessary to reconstruct the $\Xi^-$ tracks without human eyes, because the number of events to be analyzed becomes ten times more than that of E373, *i.e.* at least $2\times10^5$ events. And furthermore, image of $\Xi^-$ hyperon tracks is broader than the diameter of one fiber, so that the reconstructed angles have large errors of about 100 mrad. For each tagged event, the mean number of the $\Xi^-$ candidate tracks found in the emulsion is, therefore, more than one even by using such fine fibers.

Therefore, we will employ double-sided Si strip detector (DSSD). The ionization of the $\Xi^-$ hyperon which can stop in the emulsion is much larger than that of minimum ionizing particles. Such $\Xi^-$ hyperons give enough energy deposit in a DSSD of the thickness of 300 $\mu$m. We plan to use 20 $\sim$ 30 $\mu$m strip pitch DSSD to obtain high position resolution. Two DSSD's are installed between the target and the emulsion to measure the angle and position of $\Xi^-$ hyperons, so that we allow only one candidate track in the emulsion. Since the

resolution of deposit energy by charged particles is much better than fiber scintillator, the selection of $\Xi^-$ hyperons which can stop in the emulsion and separation from other particles like pions will be much more improved. We also will install two DSSD's downstream of the emulsion stack to determine whether the $\Xi^-$ stops in the emulsion or passes through it and to provide the additional event identification capability. We can, thus, reduce the number of events to be scanned by about one order of magnitude with use of the DSSD's.

### 3.4.2 Scintillating fiber (SCIFI)

The scintillating fiber (SCIFI) detector has been developed as a live target to search for the $H$ particle about ten years ago. We employ SCIFI blocks installed up- and downstream of the emulsion to measure the energy of $\pi^-$ mesons escaping from sequential weak decay of double strangeness nuclei produced in the emulsion. They are also used to find the decay topologies of $H \to \Sigma^- + p$ and $\Lambda + p + \pi^-$, if the bound $H$ particle exists, as well as to detect the decay of $\Lambda$ ($\Sigma$) via $\Lambda\Lambda$ weak interaction of $\Lambda\Lambda \to \Lambda(\Sigma)N$ [26]. Schematic drawings are shown in Fig. 6 and 7. The cross section of each fiber is $0.5\times0.5\text{mm}^2$. About one hundred fiber sheets are alternately packed in the $u$ and $v$ directions in order to reconstruct tracks in three dimensions. To degrade $\pi^-$ energy, aluminum sheets with 0.3 mm thickness are inserted between each SCIFI sheet. However, the amount of material from the upstream SCIFI to the emulsion is limited to be less than 10 g/cm$^2$ in order to detect X rays around 300-400 keV with Ge detectors located outside.

An image obtained by E373 is displayed in Fig. 8. The decay topology of $\Xi^-$ is clearly understood with a tagged $K^+$ tracks. In Fig. 9, the sum of brightness of the fibers along $\pi^-$ or proton tracks measured in E373 is presented in both of the up and down SCIFI blocks [27]. The identification of particles stopped in SCIFI has been well carried out. The SCIFI detector worked quite successfully at the particle rate of $10^5$ Hz in the previous KEK experiments.

The same quality of SCIFI data is expected in the proposed experiment.

## 3.5 Nuclear emulsion

The emulsion stack as shown in Fig. 3 consists of 11 thick emulsion plates and one thin plate with each cross section of $35\times35$ cm$^2$. One thin plate has 70 $\mu$m thick emulsion on both sides of 200 $\mu$m thick polystyrene base. In this thin plate, the $\Xi^-$ tracks are searched for according to the prediction by the $\Xi^-$ tracking detector (DSSD). This scanning will be done by the fully automated scanning system developed in E373. In a thick plate, emulsion of 500$\mu$m thickness is coated on both sides of polystyrene base with the thickness of 40 $\mu$m. These bases were successfully preprocessed on its both surfaces by an atmosphere pressure Corona-discharge method so that the emulsion did not separate from the base. More than one thousand plates were successfully prepared in E373 [28].

The emulsion crystal (AgBr) have been developed to get better position resolution. In the proposed experiment, we use the emulsion with fine and uniform crystal of the size of $0.18\pm0.015\mu$m, which was improved from that used in E176 ($0.24\pm0.078\mu$m).

The emuslion stack should be mechanically moved at the beam line by an emulsion mover. When the emulsion stack is installed in the beam line, its left-bottom position is set on the beam center. Firstly $y$ coordinate (vertical direction) of the stack is fixed. The emulsion mover moves the stack horizontally ($x$:right diection) during 2.3 seconds between two spills. Its driving lengh is calculated to irradiate the beam uniformly by counting exposed number of beam particles in the spill before driving. At the end of horizontal movement of 33 cm, the stack is shifted vertically about 5mm. And then the emulsion mover drives the stack horizontally, but in the opposite direction. By this method, the emulsion stack was driven in the $33 \times 32$ cm$^2$ area with a position accuracy about 10 $\mu$m. If we obtain $2 \times 10^5$ $K^-$ / spill(4.1sec), it takes 7.8 hours for the full beam exposure on one emulsion stack.

### 3.6 Ge detector

Hyperball is a large-acceptance Ge detector array dedicated to hypernuclear $\gamma$ spectroscopy [9, 29]. It is designed to work efficiently under sever counting-rate conditions at secondary hadron beams.

In the proposed experiment, we install twelve coaxial Ge detectors with a 70 mm $\phi \times$ 70 mm crystal (60% relative efficiency) for each and cover the upstream hemisphere of the target. The distance from the emulsion center to the Ge detector endcap is 15 cm. We will modify the BGO detector shape so that we can install Ge+BGO detectors as many as possible in the hemisphere in more compact arrangement. Including photon absorption in the emulsion stack and the SCIFI blocks, the photo-peak efficiency is expected to be 4% at 350 keV.

Each Ge detector is surrounded by six BGO counters, which are used to suppress Compton scattered events in the Ge crystal and high energy photons from $\pi^0$. It is confirmed that the BGO counters reduce Compton background from 1 MeV photons by a factor of 4, and reject $\pi^0$ induced background by a factor of 20 or more. Hyperball is equipped with fast readout electronics so that it works well with beam intensity even more than $1\times10^6$ mesons per second. The present beam intensity gives not effect to the detector performance; we expect no deterioration of the energy resolution ($\sim$3 keV FWHM) and no gain shift due to the beam. However, as we need precise measurement of absolute photon energy, we will monitor the in-beam performance of the Ge detectors during the whole beam time using triggerable $^{22}$Na $\beta - \gamma$ sources embedded in plastic scintillation counters. Absolute energy calibration with various $\gamma$-ray standard sources will also be frequently (more than once a day) carried out. We can thus calibrate the absolute energy scale within $\pm$0.1 keV at 350 keV. The absolute photo-peak efficiency will also be obtained by calibration with the standard source and the in-beam dead time measurement with the triggerable $^{22}$Na sources, after a correction for

the target absorption with a simulation. The absolute efficiency will be determined within $\pm 5\%$ accuracy.

The Ge detectors are cooled with liquid nitrogen, which is supplied by a automatic supply system to the Dewar tank of each Ge detector.

## 3.7 Analysis

### 3.7.1 track reconstruction and event selection

After the selection of ($K^-$,$K^+$) reaction events from the diamond target by the analysis of the spectrometer data, $\Xi^-$ tracks are searched and reconstructed in the DSSD. By using the downstream DSSD and SCIFI, candidate events of the stopping $\Xi^-$ are selected by the energy deposit in the upstream DSSD and event topologies in the downstream DSSD and SCIFI. A $\pi^-$ track reconstruction in the downstream DSSD and SCIFI block is necessary for the rejection of $\Xi^-$ decay events. Since the energy of such $\pi^-$ mesons is mostly much larger than that of the $\pi^-$ from the decay of a hypernucleus, $\Xi^-$ decay events can be rejected with use of DSSD and SCIFI. This event selection is very important, because the number of $\Xi^-$-decay events is expected to be about 10 times larger than that of stopping $\Xi^-$ events according to a Monte Carlo simulation.

We can also reject those events with $\Xi^-$ hyperon passing through the emulsion stack without stopping, by identifying a $\Xi^-$ track in the downstream DSSD and (SCIFI block).

### 3.7.2 emulsion, DSSD and SCIFI image scanning

We will trace the $\Xi^-$ candidate track found in the first emulsion plate up to its stopping point. In the $\Xi^-$ stopping point, the decay topology is measured precisely. When we find (sequential) weak decay of a double- or single-$\Lambda$ hypernucleus, all decay products should be traced up to those end points in order to measure their energies and to study characteristics of the stopping points. Particle identification should be tried by measurement of change of $I/I_0$ (energy loss ratio to minimum ionizing particle). With the downstream DSSD, one can trace a track back to the emulsion from downstream, if necessary. It may enhance the physics capability such as the decay-mode study of $S = -2$ nuclei and the $\Lambda\Lambda$-resonance search.

In the E373 experiment, the tracks reconstructed in the fiber-bundle tracker are full-automatically scanned in the first emulsion plate by the computer-aided emulsion scanning system [15, 30]. The number of found tracks in emulsion is nearly 3 times larger than the number of the predicted tracks due to the limited resolution of the fiber-bundle tracker. We follows those tracks, plate by plate, by human eyes with a guidance of the computer-aided system until their end points. About 40 % of those tracks go through the final emulsion plate, even after we cut such bad events using track images in the downstream SCIFI. The time

| | Events | Tracks[bundle] | Tracks[emulsion] | Through |
|---|---|---|---|---|
| [E373] | | | | |
| | 508 (1) | 668 (1.3) | 2004 (3.9) | 760 (1.5) |
| [proposed experiment] | | | | |
| | (1) | (1.3) | (1.3) | (0) |

Table 2: Number of tracks traced in emulsion for a sample of E373 data and expected number in the proposed experiment. Events, Tracks[bundle], Tracks[emulsion] and Through are the number of stopping $\Xi^-$ candidate events, of reconsturucted tracks in the fiber-bundle, of found tracks in the first emulsion plate and of tracks passing through the emulsion stack, respectively. Their ratios are also shown in parentheses. In the second row, expected ratios in the proposed experiment are listed.

necessary to trace such penetrating tracks is about 60% of the total time for the emulsion analysis. In table 2, the result of tracing tracks for a sample of E373 data is shown. In this method, however, all of the emulsion can be scanned within two years in E373.

In the proposed experiment, the candidate track can be detected uniquely at the first emulsion plate, because the DSSD's have much better resolution of the position and the angle for the $\Xi^-$ tracks. By detecting true $\Xi^-$ tracks at the first emulsion plate, we don't need to follow the tracks with their end point out of the emulsion, as listed in "Through" in table 2. Thus, the total number of tracks to be scanned is considerably reduced. By this reduction, the scanning of $\Xi^-$ candidate tracks is expected to be done 4 times faster than that in E373. Besides that, we will improve the softwere for the automatic scanning. The current software needs support of human eyes in decision of connected tracks between the emulsion plates. In that process, we will introduce a method of pattern matching of beams in the emulsion so that it will be mostly free from human eyes. This development will realize a reliable scanning by 2$\sim$3 times faster than that of the current one. Therefore, the scanning of the emulsion plates can be done by about one order faster than E373, and we will finish the scanning of all of the stopping $\Xi^-$ candidate tracks within a few years.

### 3.7.3 Ge detector

After the energy calibration and gain drift correction, if necessary, the photon energy spectrum will be summed up for all the Ge detectors. The BGO counter veto will be also applied to each of the Ge detectors. Then the $\Xi^-$ stopped events identified in the emulsion analysis will be selected.

Since the $\Xi$-nucleus energy shift is expected to be less than a few keV, identification of $Z$ (Ag or Br) for the observed photon peaks is trivial. Using the absolute efficiency curve, the branching ratio per $\Xi^-$ stop will be derived for each X ray peak. The absolute efficiency curve of Hyperball in the previous experiment is shown in Fig.10. The measured efficiency

curve using standard sources is well reproduced by a simulation, which indicates that the absolute efficiency in the proposing experiment will also be obtained within ±3% accuracy in the same manner.

# 4 Yield estimation to obtain $10^4$ $\Xi^-$ stop events

## 4.1 Maximum number of exposed $K^-$ particle for one stack :$n_{K^-}$

Since the emulsion records all the changed particles during exposure, the maximum number of exposed beam particles is limited. That is given as follow;

$$n_{K^-} = n_e \cdot r_s \cdot s \cdot r_{K^-}$$

where

| | | |
|---|---|---|
| $n_e$ | = | maximum number of changed particle in emulsion<br>to recognize thin tracks. $\Rightarrow 10^6/cm^2$ |
| $r_s$ | = | damage by shower particles produced<br>in the diamond target. $\Rightarrow 1/1.14$ given by Monte Carlo. |
| s | = | cross section of emulsion stack. $\Rightarrow 33 \times 32$ cm$^2$ |
| $r_{K^-}$ | = | $K^-$ ratio in beams $\Rightarrow 0.9$ (assumed) |

It is found to be able to expose $K^-$ of $8.34 \times 10^8$ ( $= n_{K^-}$) to one emulsion stack.

## 4.2 Yield of $\Xi^-$ stop in one emulsion stack : $y_{\Xi stop}$

We estimated the yield of stopping $\Xi^-$ event in the emulsion. The yield depends on the acceptance of the spectrometer and on the distance from the target to TOF counter. The yield estimation is based on the parameters of the KURAMA spectrometer in E373. The $\Xi^-$ stopping yield is written by

$$y_{\Xi stop} = y_{K^+} \cdot \eta_\Xi \cdot R_{stop}$$

where

| | | |
|---|---|---|
| $\eta_\Xi$ | = | $\Xi^-$escaping ratio from target nucleus,<br>i.e. $^{12}$C of diamond.<br>$\Rightarrow 0.8$ from the previous experiments [31] |
| $R_{stop}$ | = | $\Xi^-$stopping probability in the emulsion stack<br>estimated by Monte Carlo.<br>$\Rightarrow 0.017$(KURAMA) |

Momentum spectrum of tagged $\Xi^-$ hyperons by the spectrometer using KURAMA magnet was simulated as shown in Fig. 11 together with that of $\Xi^-$ stopped in the emulsion.

$y_{K^+}$ is the number of tagged $K^+$ in one stack exposure which is written as follow;

$$y_{K^+} = \frac{d\sigma}{d\Omega_L} \cdot \Delta\Omega \cdot N_p \cdot \eta_{abs} \cdot \eta_{K^+} \cdot \eta_{eff} \cdot n_{K^-}$$

where

| | | |
|---|---|---|
| $\frac{d\sigma}{d\Omega_L}$ | = | the cross section of quasi-free '$p$'($K^-$,$K^+$)$\Xi^-$ reaction. $\Rightarrow 50 \times 10^{-30}$ cm$^2$/ str. |
| $\Delta\Omega$ | = | acceptance of the spectrometer. $\Rightarrow$ 0.20 sr (KURAMA) |
| $N_p$ | = | effective proton number of the 3 cm long diamond target (10 g/cm$^2$). $\Rightarrow 1.36 \times 10^{24}$ |
| $\eta_{abs}$ | = | beam absorption rate in the diamond target. $\Rightarrow$ 0.947 |
| $\eta_{K^+}$ | = | detection rate of $K^+$ without decay before reaching the TOF. $\Rightarrow$ 0.735(KURAMA) |
| $\eta_{eff}$ | = | reconstruction efficiency of the tagged $K^+$. $\Rightarrow$ 0.70 is assumed. |

Finally, $y_{\Xi stop}$ is estimated to be 75.1 $\Xi^-$ stops in one stack when we use the KURAMA magnet.

## 4.3 Emulsion volume and Beam time

The volume of one stack of the emulsion is 1372 cc. To get $10^4$ $\Xi^-$ stop events, we need the emulsion volume of

$1372 \times 10000/75.1 = 183$ liters,

and 133 stacks in total. This emulsion volume is more than twice of that used in our previous E373 experiment, 70 liters (100 stacks). The total number of $K^-$ we expose is $1.1 \times 10^{11}$. If we get almost pure $K^-$ beam with an intensity of $2 \times 10^5$ $K^-$/spill (4.1 sec), we require 1100 hours beam time in total including the time for the exchange of emulsion stacks, where 7.8 hours and $\sim$ 0.5 hours are necessary for the beam exposure on one emulsion stack and the exchange, respectively. The beam time should be divided into two years, 550 hours in each year, because of time necessary for emulsion development as described later. We request beam time of 750 hours for the first year and 650 hours for the second year, which includes the time to test all the detectors (100 hours each year) and to study beam profile and quality (100 hours only in the first year).

| $Z(n,l)$ | $E$ (keV) | $y_{\Xi\text{stop}}$ | $\epsilon_{\text{Ge}}$ | $R_X$ (case 1) | $y_{\Xi\text{X}}$ | accuracy(keV) $\pm$stat.$\pm$syst. | shift (case 1) | shift (case 2) |
|---|---|---|---|---|---|---|---|---|
| Ag(8,7)$\rightarrow$(7,6) | 370.45 | 3400 | 0.038 | 0.88 | 114 | $\pm$0.12$\pm$0.10 | 0.28 | 3.3 |
| Br(7,6)$\rightarrow$(6,5) | 315.5 | 2500 | 0.044 | 0.73 | 80 | $\pm$0.15$\pm$0.10 | 0.73 | 5.5 |

Table 3: Expected yields of $\Xi$ atomic X rays and accuracy of the X-ray energy measurement. See Table 1 for the case 1 and the case 2 of the $\Xi$ X-ray calculation.

## 4.4 Yield of X rays with Hyperball

In E176, the number of observed events of $\Xi^-$ absorption on the heavy nuclei (Br and Ag) was 47$\pm$5 and that on the light nuclei (C,N,O) was 31$\pm$5 in total 80 events of stopped $\Xi^-$. Considering the atomic ratio of Br:Ag=1:1 and assuming the $Z$ dependence of the atomic capture ratio, Br:Ag=35:47, then the numbers of identified stopped $\Xi^-$ events $y_{\Xi\text{stop}}$ on Br and Ag is 2500 and 3400 in the total $1\times10^4$ stopped $\Xi^-$ events.

The number of X-ray events is derived as

$$y_{\Xi\text{X}} = y_{\Xi\text{stop}}\ \epsilon_{\text{Ge}}\ R_X$$

where $\epsilon_{\text{Ge}}$ is the photo-peak efficiency of Hyperball at the X-ray energy, and $R_X$ is the branching ratio of this transition per $\Xi^-$ absorption. The accuracy of the energy shift of the X ray has a statistical error calculated as $\Delta E/\sqrt{y_{\Xi\text{X}}}$, where $\Delta E$ is the energy resolution of the Ge detectors at this energy ($\sim$ 1.3 keV rms or 3.1 keV FWHM). The systematic error from the calibration of the absolute energy will be about $\pm$0.1 keV.

As shown in Table 3, the accuracy of $\pm$0.2 keV will be achieved for the absolute energy of the X rays. This accuracy is good enough compared with the predicted energy shifts in Table 1.

In the estimation of the accuracy of the energy shift, we assumed that effect of the background in the photon spectrum is negligible. Possible backgrounds are only $\gamma$-rays emitted after $\Xi^-$ absorption followed by formation of excited nuclear fragments. Several $\gamma$ rays from various nuclei may be emitted per each $\Xi^-$ stop event. Considering the energy resolution and peak-to-Compton ratio of the Ge detectors and also the Compton suppression effect by the BGO counters, we can safely expect that the background level in the Ge detector energy spectrum will be of the order of 0.1 events per keV at around 350 keV. It gives no effect to the sensitivity of the energy measurement of the X ray peak consisting of 80 or 114 events.

It is also noted that a possibility of confusion between the $\Xi$ atomic X ray and any nuclear $\gamma$ ray is expected to be very small, considering the energy resolution of 3 keV and a possible X-ray shift less than a few keV.

### 4.5 Emulsion handling

In the E373 experiment, we made 100 stacks of the emulsion plates, by pouring emulsion gel on the base plates and drying it. It took 7 months in total by three people at Gifu University. This plate-making speed is limited by the number of the drying machines. Since the size of the emulsion plate is larger than in E373 and we will prepare two drying machines, we will be able to make all of the emulsion plates in four months. We request a room for the emulsion pouring at BNL.

We must develop the emulsion as soon as possible after the beam exposure, because latent images fade away in time. According to our experience in E373, if the exposed emulsion is stored at a low temperature of $5^oC$, the enough number of developed grains is obtained for minimum ionizing particles within 5 months after the beam exposure. By separating the beam time into two years, we can develop all the exposed emulsion in 5 months in each year. Additionally, the emulsion accumulates all the charged particles not only from beam interactions but also from cosmic rays. Assuming that we send exposed emulsion to Japan by air, tracks with a density of several$\times 10^4$ /cm$^2$ might be recorded. Therefore, to expose the beam up to the limit and to develop the emulsion soon after the exposure, we request a room for the emulsion development facility at BNL.

## 5 Summary

We propose an experiment for systematic study of nuclear systems with double strangeness by using a new emulsion-counter hybrid method. The emulsion is used to detect especially hyperfragments and to identify formation and decay of $\Xi^-$ atoms. Counters are used to identify ($K^-$,$K^+$) reaction and $\Xi^-$ emission, and to measure energies of X rays from $\Xi^-$ atoms.

About ten years ago, the 1st generation hybrid emulsion experiment, KEK-E176, found that double strangeness nuclei are efficiently produced through $\Xi^-$ nuclear capture at rest (stopping $\Xi^-$ events in the emulsion). In order to obtain ten times more stopping $\Xi^-$ events, the 2nd generation experiment using an emulsion-scintillating fiber hybrid method, KEK-E373, was carried out. We have established weakly attractive $\Lambda\Lambda$ interaction by observation of an uniquely identified ${}^{\ 6}_{\Lambda\Lambda}$He event.

The goal of the proposed experiment is to obtain $10^4$ stopping $\Xi^-$ events in emulsion, which will provide one thousand events showing formation of double strangeness nuclear systems. Among them, we will identify one hundred nuclear fragments with double strangeness and make a chart of $S$=-2 nuclide.

The objective of the experiment is a systematic measurement $S$=-2 nuclei and to determine their binding energies, especially ($A$) dependence of the '$\Lambda\Lambda$ interaction energy' for, at least, several nuclides.

If a $H$ dibaryon state exists in nuclei, study of not only the $A$ dependence of the $\Lambda\Lambda$ interaction energy but also decay modes of double strangeness nuclei will clarify the existence of such a $H$ dibaryon state.

Since the number of stopping $\Xi^-$ events is ten times more than in E373, the sensitivity of the present experiment will be greatly improved for double strangeness nuclei, the $H$ dibaryon and also $\Xi^-$ atoms. By selecting stopping $\Xi^-$ events in emulsion analysis, we precisely measure the energies of X rays from $\Xi^-$ atoms on Ag and Br nuclei using Ge detectors. The enegy shifts and yields of X rays will provide definite information on the $\Xi$-nucleus potential and then the $\Xi N$ interaction.

In order to improve statistics by ten times, we take advantage of almost pure $K^-$ beam obtained at the D6 beam line, which is compared to $K^-/\pi^- \sim 1/4$ at KEK. We employ a new high position resolution detector, double-sided Si strip detector, to reconstruct $\Xi^-$ tracks rather than scintillating fiber bundle used in E373 in order to make the time-consuming emulsion scanning easier and faster. They are essential to observe $10^4$ stopping $\Xi^-$ events in the emulsion. The scintillating fiber blocks which surround the emulsion are used to detect $\pi^-$ and higher energy particles, and the emulsion is used to detect mainly hyperfragments. The Ge detectors will catch X rays from $\Xi^-$ atomic orbits.

Various new techniques developed in our previous experiments will be combined in this experiment. It is, technically, the third generation experiment of this kind.

# References


[1] M. Danysz et al., Nucl. Phys. **49** (1963) 121.

[2] R.H. Dalitz et al., Proc. R. Soc. Lond. **A426** (1989) 1.

[3] P.J. Prowse, Phys. Rev. Lett. **17** (1966) 782.

[4] S. Aoki et al., Prog. Theor. Phys. **85** (1991) 1287.

[5] K. Nakazawa, KEK proposal E373 (1995); K. Nakazawa, Nucl. Phys. **A585** (1995) 75c; *ibid.* **A639** (1998) 345c.

[6] A. Ichikawa et al., Nucl. Instr. & Meth. **A417**(1998)220.

[7] A. Ichikawa et al., Phys. Lett. **B500** (2001) 37.

[8] H. Takahashi et al., submitted to Phys. Rev. Lett.

[9] H. Tamura et al., Phys. Rev. Lett. **84** (2000) 5963.

[10] H. Akikawa et al., Nucl. Phys.**A691** (2001) 134.

[11] K. Tanida et al., Phys. Rev. Lett. **86** (2001) 1982.

[12] R. L. Jaffe, Phys. Rev. Lett. **38** (1977) 195.

[13] D. Zhu et al., Phys. Rev. Lett. **67** (1991) 2268.

[14] C. J. Batty, E. Friedman and A. Gal, Phys. Rev. **C59** (1999) 295.

[15] A. Ichikawa, Ph.D. thesis, Kyoto University (2001), (unpublished).

[16] J. K. Ahn et al., the proceedings of Hadron & Nuclei, in Seoul (Feb. 2001), AIP press, to be published.

[17] R. E. Chrien, Nucl. Phys. **A629** (1998) 388c; B. Bassalleck, Nucl. Phys. **A639** (1998) 401c; R. E. Chrien, Nucl. Phys. **A691** (2001) 501c.

[18] J. K. Ahn et al., Phys. Lett. **B444** (1998) 267.

[19] T. Yamada and C. Nakamoto, Phys. Rev. **C62** (2000) 034319; T. Yamada, Nucl. Phys. **A691** (2001) 250c.

[20] T. Yamada, private communications (2001).

[21] Y. Yamamoto, Few-Body Systems Suppl. **9** (1995) 145; T. Fukuda et al., Phys. Rev. **C58** (1998) 1306; P. Khaustov et al., Phys. Rev. **C61** (2000) 054630.

[22] C.J. Batty, E. Friedman and A. Gal, Phys. Lett. **B335** (1994) 273 and references therein.

[23] E. Friedman and A. Gal, private communications (2001).

[24] S. Aoki et al., Prog. Theor. Phys. **89** (1993) 293.

[25] S. Aoki et al., Phys. Lett. **B335** (1995) 45.

[26] K. Itonaga, T. Ueda, T. motoba, Nucl. Phys. **A691** (2001) 197c; A. Parreno, proceedings of *Mesons & Light Nuclei*, Prague, July 2001, AIP press, to be published.

[27] H. Takahashi et al., Nucl. Instr. Meth. **A417** (2001) in print.

[28] H. Akikawa et al., to be submitted to Nucl. Instr. Meth. **A**.

[29] K. Tanida, Ph.D. thesis, University of Tokyo, 2000.

[30] A. Ichkawa et al., to be submitted to Nucl. Instr. Meth. **A**.

[31] S. Aoki et al., Nucl. Phys. **A644** (1998) 365.

## List of collaborators

| | |
|---|---|
| Kyoto University: | H. Funahashi, K. Imai, M. Nakamura, graduate students |
| Gifu University: | M. Mitsuhara, K. Nakazawa, K. Ohashi, graduate students |
| Tohoku University: | Y. Miura, K. Mizunuma, H. Tamura, M. Ukai, graduate students |
| BNL: | R.E. Chrien, H. Hotchi, M. May, P. Pile, A. Rusek |
| CIAE: | H. Gue, Z. Liu, S. Lu, J. Zhou |
| Carnegie Mellon University: | G.B. Franklin, graduate students |
| Geyongsang National University: | B.D. Park, I.G. Park, J.S. Song, C.S. Yoon, graduate students |
| University of New-Mexico: | B. Bassalleck, graduate students |
| Osaka City University: | K. Yamamoto, T. Yoshida, graduate students |
| Pusan National University: | J.K. Ahn, S.J. Kim, graduate students |
| RIKEN: | K. Tanida |

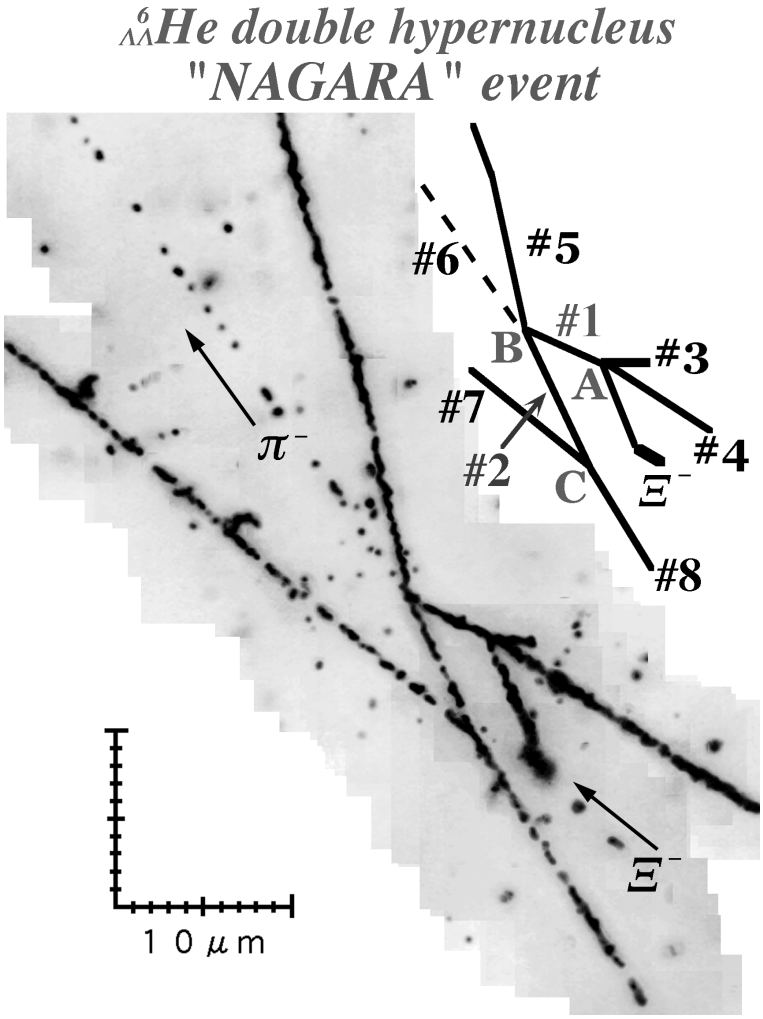


Figure 1: NAGARA event showing production and decay of *Lambpha* ($^{6}_{\Lambda\Lambda}$He double hypernucleus) observed in E373. A $\Xi^-$ hyperon is captured by a $^{12}$C nucleus at the point A, and a double hypernucleus (#1) and two stable nuclei are emitted. At the point B, track #1 decays to #2 (single-$\Lambda$ hypernucleus), #5 and #6. Track #7 and #8 are decay daughters of #2 from the point C. #6 can be identified as $\pi^-$ by its characteristic topology at the end point in the emulsion. Track #7 is escaping from the emulsion stack. By the analysis of brightness of the track in SCIFI block, it was recognized that the track cannot be $\pi^-$. This event is uniquely identified as: $\Xi^-+{}^{12}\mathrm{C} \rightarrow {}^{6}_{\Lambda\Lambda}\mathrm{He}+{}^{4}\mathrm{He}+t$, ${}^{6}_{\Lambda\Lambda}\mathrm{He} \rightarrow {}^{5}_{\Lambda}\mathrm{He}+\pi^-+p$, ${}^{5}_{\Lambda}\mathrm{He} \rightarrow p+d+2n$ *etc.*

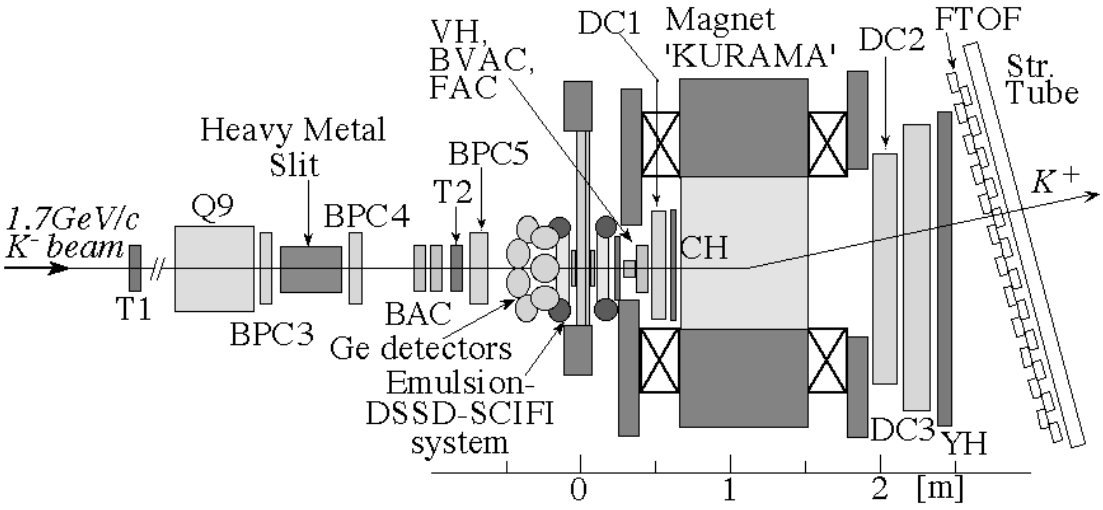


Figure 2: The setup of the present experiment (top view).

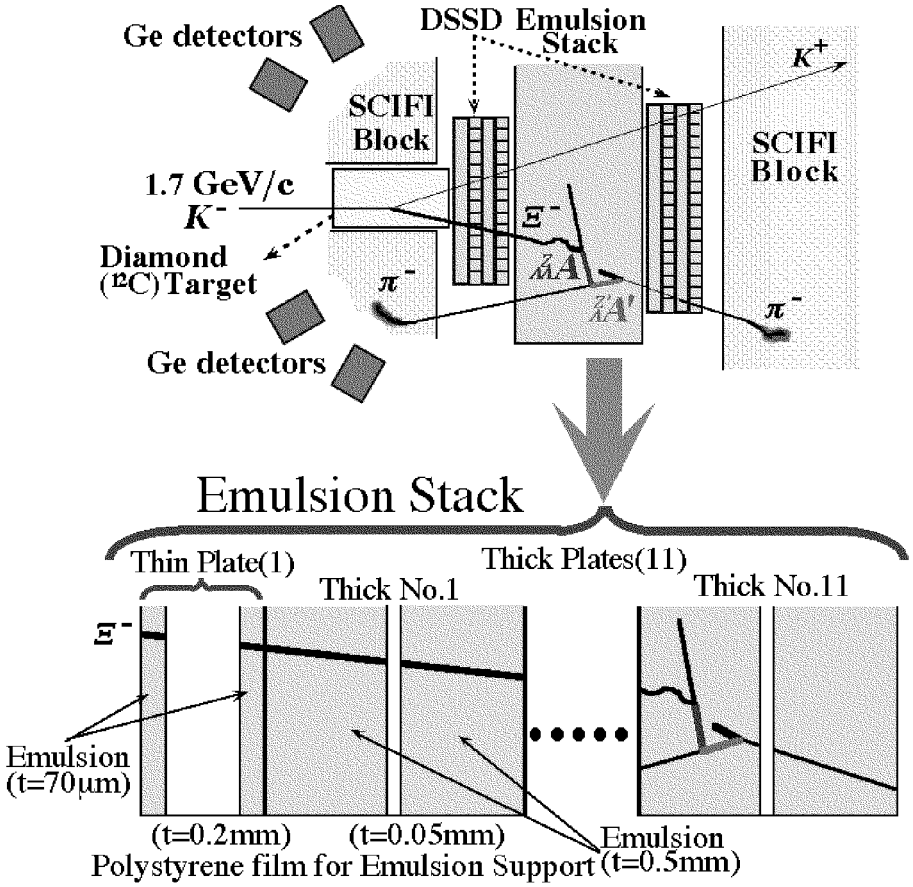


Figure 3: The apparatus around the emulsion and the emulsion stack.

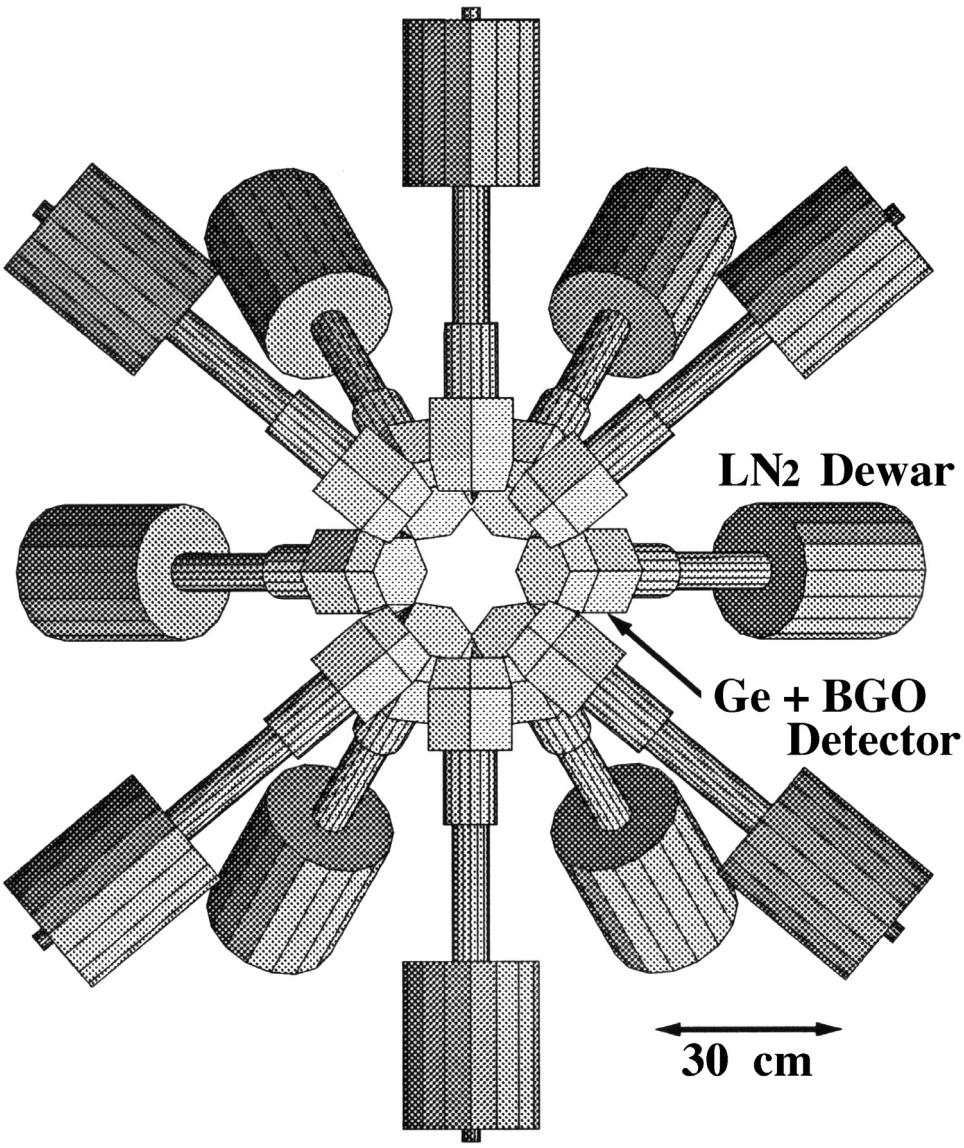


Figure 4: Setup of Hyperball viewed from downstream to upstream. Twelve sets of Ge+BGO detectors are installed upstream hemisphere around the target region (the target, emulsion and SCIFI are not shown).

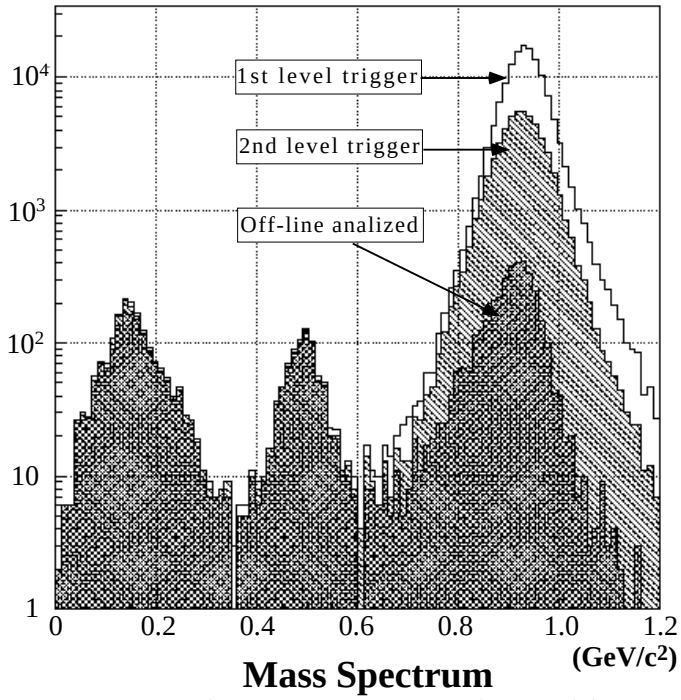

Figure 5: The mass spectrum obtained by E373.

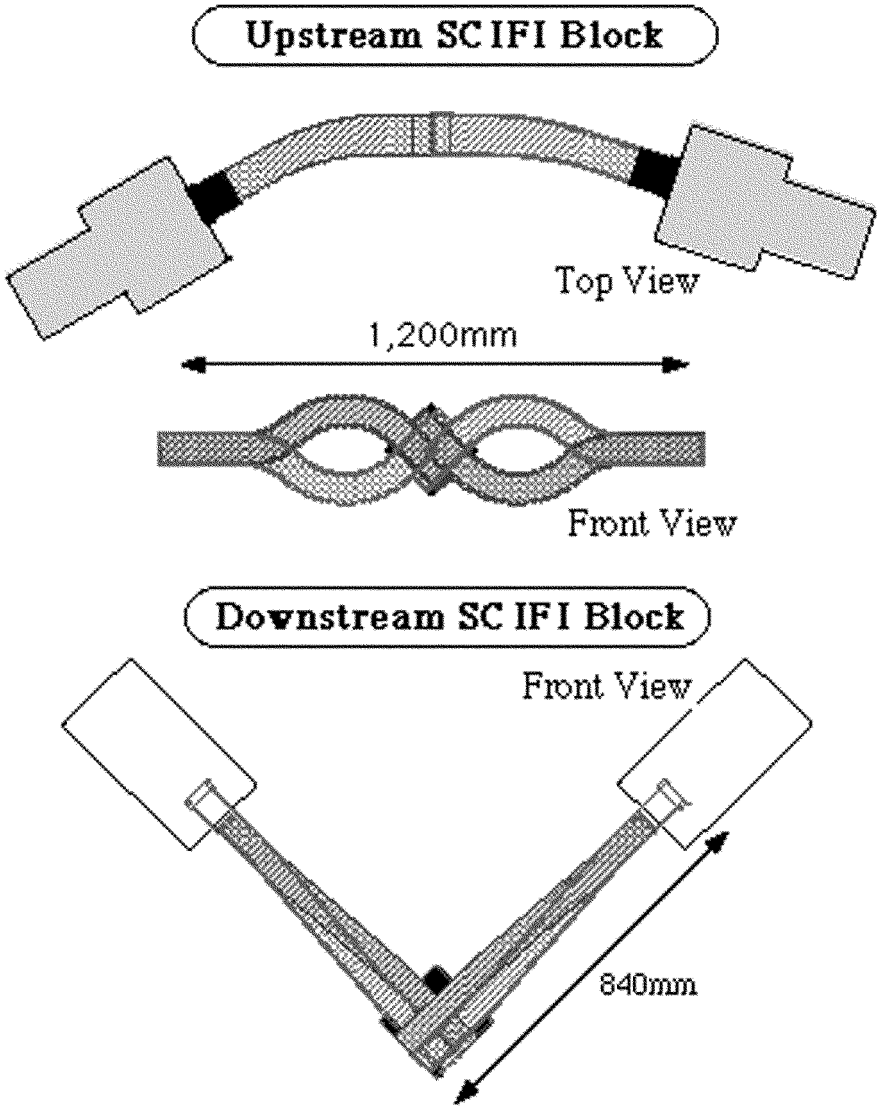


Figure 6: Schematic drawings of the SCIFI blocks.

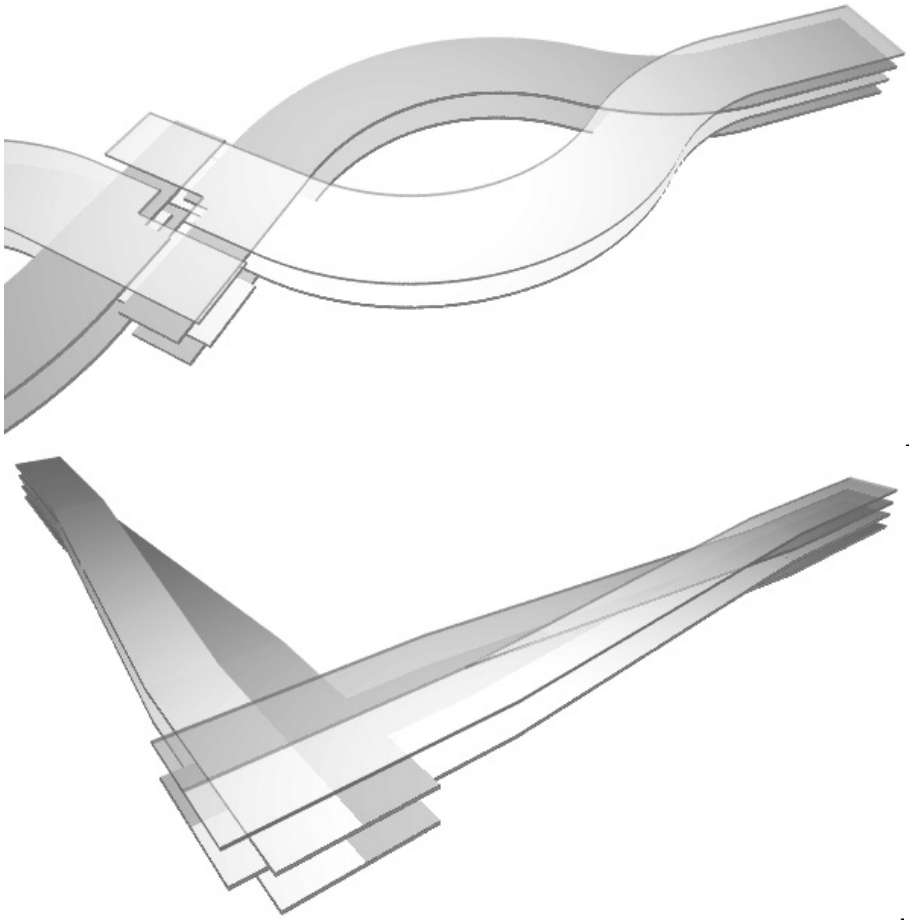

Figure 7: Concept of upstream and downstream SCIFI blocks.

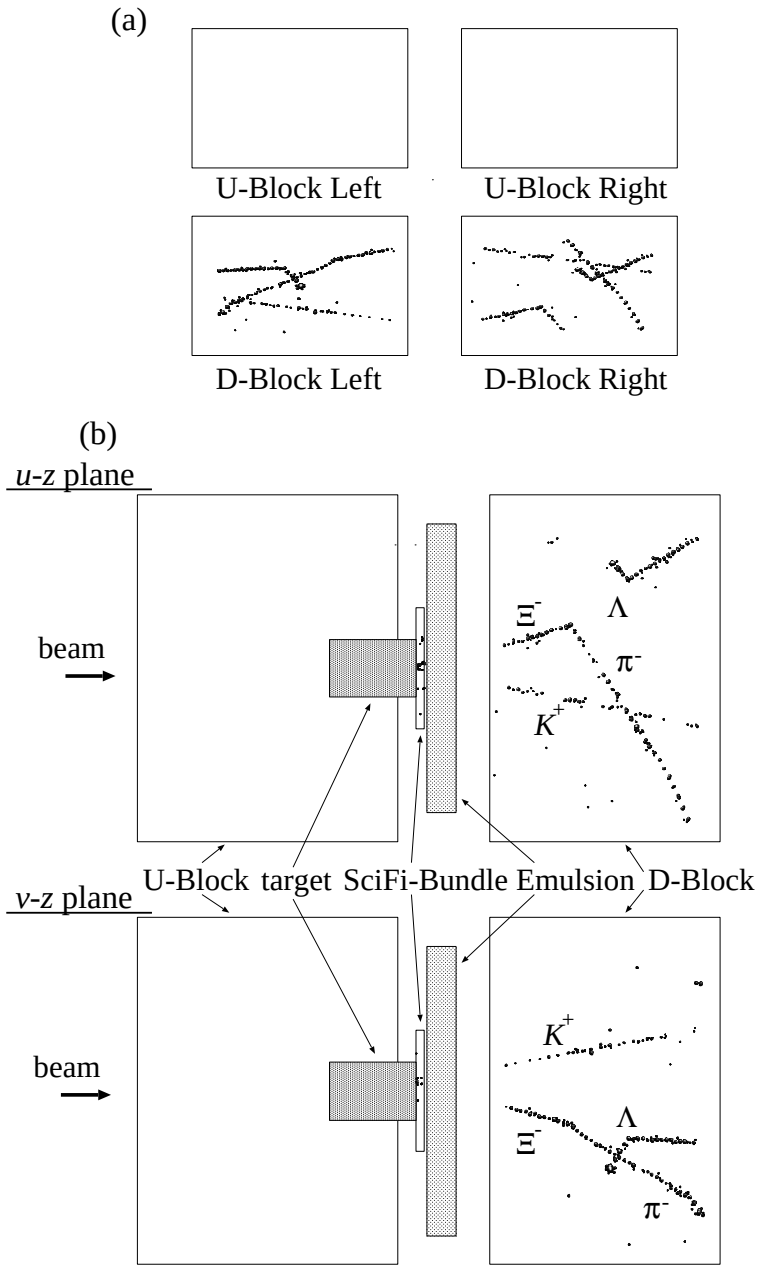


Figure 8: An image of $\Xi^-$ decay sequence shown in SCIFI blocks in E373.

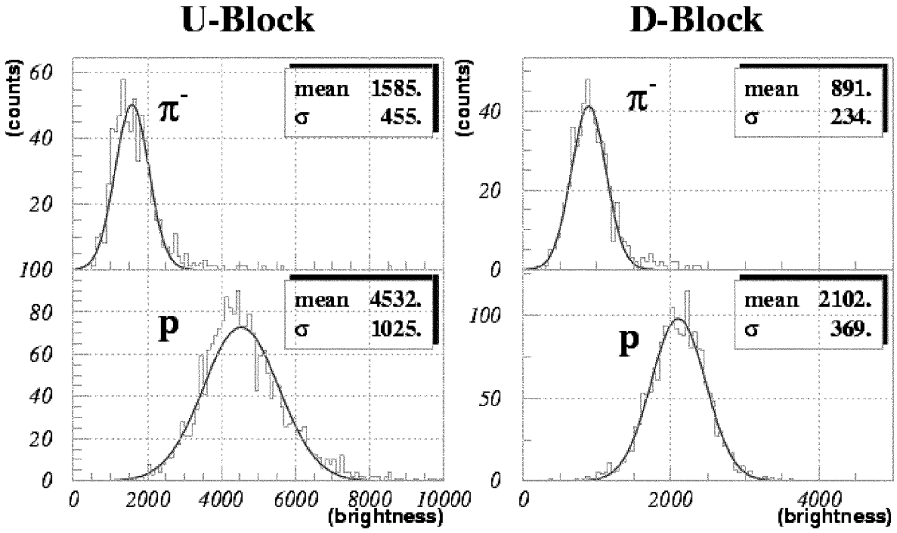


Figure 9: Brightness for stopped $\pi^-$ and proton in SCIFI blocks obtained by E373.

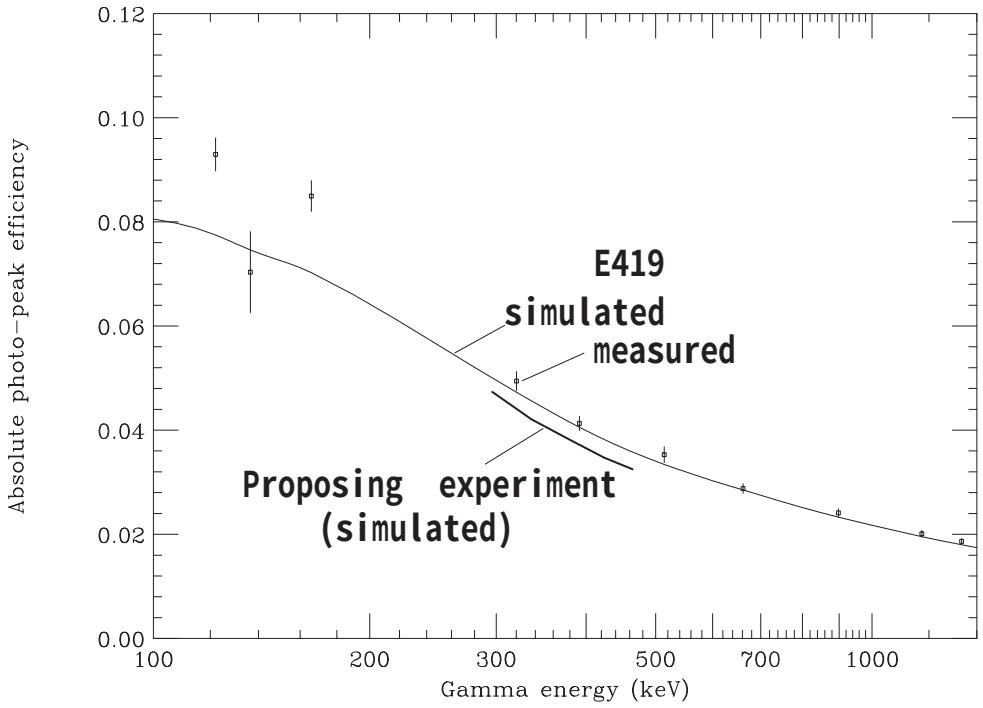


Figure 10: Photo-peak efficiency of Hyperball in the proposed experimental setup using 12 Ge detectors in the half hemisphere. The efficiencies in the E419 experiment (measured and simulated) using the full set of Hyperball are shown together.

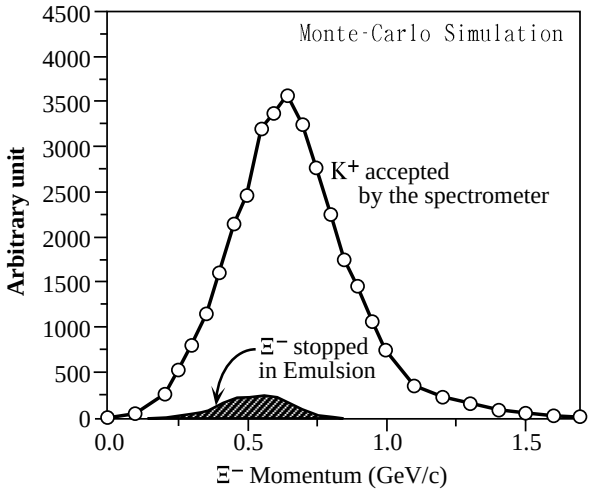


Figure 11: Momentum spectrum of $\Xi^-$ tagged by the spectrometer and stopped in emulsion (Monte Carlo simulation).